J|A|C|S ARTICLES

Published on Web 03/10/2010

Relation between Serum Amyloid A Truncated Peptides and Their Suprastructure Chirality

Noa Rubin,[†] Emanuel Perugia,[‡] Sharon G. Wolf,[§] Eugenia Klein,[§] Mati Fridkin,[‡] and Lia Addadi*,[†]

Department of Structural Biology, Department of Organic Chemistry, and Irving and Cherna Moskowitz Center for Nano and Bio-Nano Imaging, Weizmann Institute of Science, Rehovot, Israel 76100

Received November 4, 2009; E-mail: lia.addadi@weizmann.ac.il

Abstract: Amyloids are pathological fibrillar aggregates of proteins related to over 20 diseases. Amyloid fibers are characterized by the cross-β motif, which is minimally defined as a series of β-strands extended perpendicular to the fiber axis, joined by hydrogen bonds parallel to the fiber direction. Several structures, all in agreement with the cross-β definition, have been proposed for specific amyloids. We study the correlation among the suprastructural chirality, molecular structure, and molecular chirality of amyloids. Here we investigate the suprastructure chirality of different (all-*S*) serum amyloid A (SAA) truncated peptides. We found that the suprastructure chirality of amyloid fibers from segments SAA_{2-6}, SAA_{1-11} and the majority of those from SAA_{2-9} is left-handed, which is consistent with the β-sheet protofilament model. In contrast, SAA_{1-12} and SAA_{2-12} as well as SAA_{1-12}, where the C-terminal aspartic acid was point mutated to either leucine or alanine, form right-handed helical amyloid fibers. Such a suprastructure switch indicates a molecular change in the protofilament structure. This is supported by the behavior observed in the FTIR spectra, where the amide I peak of all of the right-handed fibers is red shifted relative to the left-handed amyloid fibers. This work is a case study where isolated short fragments of SAA containing the same amyloidogenic core sequence fold into different amyloid structures. We show that core sequences, supposed to start the misfolding aggregation of the full-length amyloid peptides, may have structures different from those assumed by the isolated segments.

Introduction

In the living cell, protein function is related directly to the integrity of the native structure. Conformations other than the correct functional fold may thus lead to diseases.[1] Several human diseases are associated with protein misfolding, such as amyloid diseases. Over 20 diseases have been identified as amyloid-related, among them Alzheimer's, Parkinson's, diabetes type II, Huntington disease, and the well-known prion diseases.[2,3] Each disease is associated with the deposition in a specific body organ of a polypeptide that aggregates and accumulates irreversibly in the tissue forming amyloid fibers.[4] In recent years, different studies have demonstrated that proteins not related to amyloid diseases[5,6] and even homopolypeptides[7] can form amyloid structures in appropriate physicochemical environments.

What is common to all amyloid fibers, despite the large diversity in amyloid protein sequences, is the cross-β motif. The cross-β motif is minimally defined as a series of β-strands extended perpendicular to the fibril axis, joined by hydrogen bonds parallel to the fibril direction.[4] Several protofilament structures, all consistent with the cross-β definition, have been proposed for specific amyloids, such as β-sheet, β-helix, or other β-structures.[8−18]

[†] Department of Structural Biology.
[‡] Department of Organic Chemistry.
[§] Irving and Cherna Moskowitz Center for Nano and Bio-Nano Imaging.

(1) Dobson, C. M. *Philos. Trans. R. Soc. London, Sect. B* **2001**, *356*, 133–145.
(2) Stefani, M.; Dobson, C. M. *J. Mol. Med.* **2003**, *81*, 678–699.
(3) Chiti, F.; Dobson, C. M. *Annu. Rev. Biochem.* **2006**, *75*, 333–366.
(4) Sunde, M.; Serpell, L. C.; Bartlam, M.; Fraser, P. E.; Pepys, M. B.; Blake, C. C. *J. Mol. Biol.* **1997**, *273*, 729–739.
(5) Guijarro, J. I.; Sunde, M.; Jones, J. A.; Campbell, I. D.; Dobson, C. M. *Proc. Natl. Acad. Sci. U.S.A.* **1998**, *95*, 4224–4228.
(6) Fandrich, M.; Fletcher, M. A.; Dobson, C. M. *Nature* **2001**, *410*, 165–166.
(7) Fandrich, M.; Dobson, C. M. *EMBO J.* **2002**, *21*, 5682–5690.
(8) Jimenez, J. L.; Guijarro, J. I.; Orlova, E.; Zurdo, J.; Dobson, C. M.; Sunde, M.; Saibil, H. R. *EMBO J* **1999**, *18*, 815–821.
(9) Jimenez, J. L.; Nettleton, E. J.; Bouchard, M.; Robinson, C. V.; Dobson, C. M.; Saibil, H. R. *Proc. Natl. Acad. Sci. U.S.A.* **2002**, *99*, 9196–9201.
(10) Wang, J.; Gulich, S.; Bradford, C.; Ramirez-Alvarado, M.; Regan, L. *Structure* **2005**, *13*, 1279–1288.
(11) Petkova, A. T.; Ishii, Y.; Balbach, J. J.; Antzutkin, O. N.; Leapman, R. D.; Delaglio, F.; Tycko, R. *Proc. Natl. Acad. Sci. U.S.A.* **2002**, *99*, 16742–16747.
(12) Kishimoto, A.; Hasegawa, K.; Suzuki, H.; Taguchi, H.; Namba, K.; Yoshida, M. *Biochem. Biophys. Res. Commun.* **2004**, *315*, 739–745.
(13) Perutz, M. F.; Finch, J. T.; Berriman, J.; Lesk, A. *Proc. Natl. Acad. Sci. U.S.A.* **2002**, *99*, 5591–5595.
(14) Govaerts, C.; Wille, H.; Prusiner, S. B.; Cohen, F. E. *Proc. Natl. Acad. Sci. U.S.A* **2004**, *101*, 8342–8347.
(15) Guo, J. T.; Wetzel, R.; Xu, Y. *Proteins* **2004**, *57*, 357–364.
(16) Margittai, M.; Langen, R. *Proc. Natl. Acad. Sci. U.S.A.* **2004**, *101*, 10278–10283.
(17) Wasmer, C.; Lange, A.; Van Melckebeke, H.; Siemer, A. B.; Riek, R.; Meier, B. H. *Science* **2008**, *319*, 1523–1526.
(18) Paravastu, A. K.; Leapman, R. D.; Yau, W. M.; Tycko, R. *Proc. Natl. Acad. Sci. U.S.A.* **2008**, *105*, 18349–18354.

10.1021/ja909345p

In the β-sheet protofilament model, the cross-β motif is achieved by hydrogen bonding of strands to form a β-sheet. In one protofilament, various β-sheets are stacked through intersheet interactions.[8–11] In the β-helix protofilament model, a series of single polypeptide chains in extended conformation join and revolve, forming a spiral where each turn is hydrogen bonded to the neighboring turns, yielding a pitch of 4.75 Å that results in the typical cross-β diffraction. Different helices then aggregate into fibers.[12–17] Interestingly, a recent ssNMR study has proposed a cross-β-based protofilament model for the Aβ peptide, which cannot be classified as either β-sheet or β-helix.[18] This example emphasizes that there are different protofilament β-folds, which all are in agreement with the cross-β motif.

Amyloid heterogeneity is also demonstrated in their suprastructure. When viewed under the electron microscope, amyloid suspensions are usually heterogeneous in terms of fiber morphology. Within the same sample, variable amyloid widths are observed and different morphologies, such as ribbons and helices with variable pitch, are detected.[9,19,20]

These phenomena of polymorphism may originate independently from different causes: fiber width and pitch are directly influenced by the number of protofilaments that build up the fiber.[9,21] A ribbon morphology may result from the aggregation of a large number of protofilaments. An alternative source of polymorphism, which may appear in parallel with the former, may be due to different molecular structures[22] or different overall symmetry (2-fold vs 3-fold)[18] in the protofilament architecture.

Amyloid suprastructures have been little addressed until now. It is experimentally established that (*S*)-amino acid[23] β-sheets are characterized by a left-handed twist along the sheet.[24,25] The left-handed twist along the β-sheet is attributed to the stacking of twisted β-strands, which is derived directly from the molecular chirality of the amino acids. Helical suprastructures resulting from the association of several β-sheets should subsequently also display left-handed helicity. This was both experimentally confirmed and theoretically justified.[26−30] The same does not hold true for all amyloid protofilament models. For example, β-helices were found to form both left- and right-handed helices, regardless of the chiral amino acids having only the (*S*) configuration.[14,31,32] Thus, contrary to the β-sheet suprastructures, in β-helices the molecular chirality does not translate directly into a suprastructure of defined chirality.

In a recent communication,[33] we explored the rules of organization that govern the relation between the suprastructure and the molecular structure in amyloids by studying amyloid morphology under high-resolution scanning electron cryomicroscopy (cryo-SEM). The observation that (all-S) Aβ_{1-40} and (all-S) hen lysozyme always and only form left-handed helical fibers is in agreement with the conventional β-sheet protofilament model. However, the finding that amyloids, formed by the (all-S) SAA_{1-12} peptide, always and only form right-handed helices makes it extremely unlikely that the SAA_{1-12} protofilaments assume a β-sheet structure.[33]

SAA_{1-12} is a 12 amino acid peptide (RSFFSFLGEAFD) from the N terminus of the serum amyloid A protein, which is related to secondary systemic amyloidosis (AA).[34,35]

Serum amyloid A (SAA) is a family of small proteins (12 kDa, 104−114 amino acids) associated in serum with high-density lipoproteins (HDL_3) and highly conserved in vertebrates.[36] During states of inflammation, the in vivo concentration of SAA often rises as much as 1000-fold above the normal level (up to 1 mg/mL),[37] suggesting that it might play a short-term role in host defense and tissue injury.[38,39]

A continuous high concentration of SAA for longer periods of time, induced by several chronic conditions such as autoimmune and chronic diseases, may cause disorders such as atherosclerosis and amyloidosis A (AA). Amyloidosis A is one of the most common forms of systemic amyloidosis, generated from pathological aggregation and fibril formation of the (SAA) proteins that invade the extracellular spaces of organs, destroying normal tissue structure and function.[36]

To date, structural studies on SAA using advanced methods (NMR and X-ray diffraction) have not been reported. Studies based on predictive methods suggested that SAAs are globular proteins containing two α-helix regions and a β-sheet-prone section, including the amyloid A (AA) polypeptide.[36] Amyloid A is a proteolytic product of SAA1, which incorporates 76 residues from the protein N terminus.[40] The amyloidogenic core of SAA is believed to reside in the first 12 amino acids of the protein.[35] Truncation of the N-terminus arginine results in peptide SAA_{2-12} (SFFSFLGEAFD), which also forms amyloid fibers.[35]

Here we study different truncated and mutated segments of the first 12 amino acids from the N terminus of SAA, which also form amyloid fibers under the same in vitro conditions. We show that changes in the level of one amino acid are sufficient to cause a change in the supramolecular chirality of the amyloid fibers, reflecting changes in molecular structure.

Studying the formation of small amyloidogenic regions might help in the understanding of the formation of amyloids. In addition, structural information on the short amyloid-forming

(19) Goldsbury, C. S.; Wirtz, S.; Muller, S. A.; Sunderji, S.; Wicki, P.; Aebi, U.; Frey, P. *J. Struct. Biol.* **2000**, *130*, 217–231.
(20) Serpell, L. C.; Smith, J. M. *J. Mol. Biol.* **2000**, *299*, 225–231.
(21) Jimenez, J. L.; Tennent, G.; Pepys, M.; Saibil, H. R. *J. Mol. Biol.* **2001**, *311*, 241–247.
(22) van der Wel, P. C.; Lewandowski, J. R.; Griffin, R. G. *J. Am. Chem. Soc.* **2007**, *129*, 5117–5130.
(23) By definition all L-amino acids, besides cysteine, have the S configuration.
(24) Chothia, C. *J. Mol. Biol.* **1973**, *75*, 295–302.
(25) Richardson, J. S. *Adv. Protein Chem.* **1981**, *34*, 167–339.
(26) Serpell, L. C. *Biochim. Biophys. Acta* **2000**, *1502*, 16–30.
(27) Wadai, H.; Yamaguchi, K.; Takahashi, S.; Kanno, T.; Kawai, T.; Naiki, H.; Goto, Y. *Biochemistry* **2005**, *44*, 157–164.
(28) Aggeli, A.; Nyrkova, I. A.; Bell, M.; Harding, R.; Carrick, L.; McLeish, T. C.; Semenov, A. N.; Boden, N. *Proc. Natl. Acad. Sci. U.S.A.* **2001**, *98*, 11857–11862.
(29) Soto, P.; Cladera, J.; Mark, A. E.; Daura, X. *Angew. Chem., Int. Ed.* **2005**, *44*, 1065–1067.
(30) Bellesia, G.; Fedorov, M. V.; Kuznetsov, Y. A.; Timoshenko, E. G. *J. Chem. Phys.* **2005**, *122*, 134901.
(31) Graether, S. P.; Kuiper, M. J.; Gagne, S. M.; Walker, V. K.; Jia, Z. C.; Sykes, B. D.; Davies, P. L. *Nature* **2000**, *406*, 325–328.
(32) Leinala, E. K.; Davies, P. L.; Doucet, D.; Tyshenko, M. G.; Walker, V. K.; Jia, Z. C. *J. Biol. Chem.* **2002**, *277*, 33349–33352.
(33) Rubin, N.; Perugia, E.; Goldschmidt, M.; Fridkin, M.; Addadi, L. *J. Am. Chem. Soc.* **2008**, *130*, 4602–4603.
(34) Stix, B.; Kahne, T.; Sletten, K.; Raynes, J.; Roessner, A.; Rocken, C. *Am. J. Pathol.* **2001**, *159*, 561–570.
(35) Westermark, G. T.; Engstrom, U.; Westermark, P. *Biochem. Biophys. Res. Commun.* **1992**, *182*, 27–33.
(36) Uhlar, C. M.; Whitehead, A. S. *Eur. J. Biochem.* **1999**, *265*, 501–523.
(37) Marhaug, G. *Scand. J. Immunol.* **1983**, *18*, 329–338.
(38) Manley, P. N.; Ancsin, J. B.; Kisilevsky, R. *Med. Hypotheses* **2006**, *66*, 784–792.
(39) Hari-Dass, R.; Shah, C.; Meyer, D. J.; Raynes, J. G. *J. Biol. Chem.* **2005**, *280*, 18562–18567.
(40) Yamada, T.; Liepnieks, J. J.; Kluve-Beckerman, B.; Benson, M. D. *Scand. J. Immunol.* **1995**, *41*, 94–97.

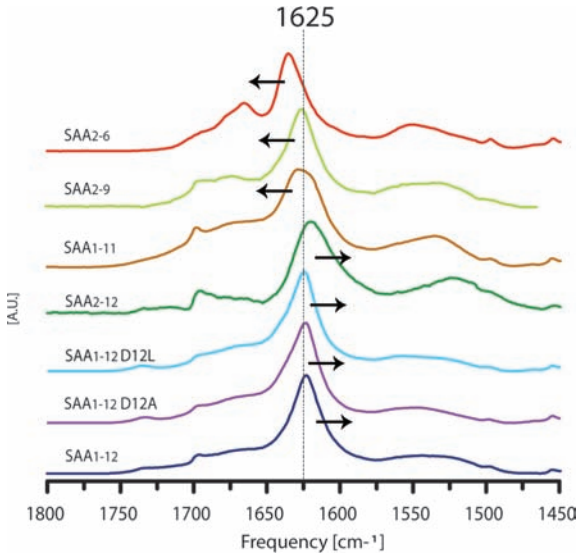

Figure 1. FTIR spectra of the amide I and II regions of SAA_{1-12} (blue), SAA_{1-12} D12A (purple), SAA_{1-12} D12L (cyan), SAA_{2-12} (dark green), SAA_{1-11} (brown), SAA_{2-9} (light green), and SAA_{2-6} (red) amyloids. All spectra are characteristic of the β-structures, although they differ from one another. The main amide I peak of SAA_{1-12} amyloids and its mutated peptides ranges from 1623 to 1625 cm^{-1} and shifts to an even lower frequency (1619 cm^{-1}, red shift) in SAA_{2-12}. In SAA_{1-11}, SAA_{2-9} and SAA_{2-6} amyloids the main amide I peak shifts to higher frequencies (blue shift) ranging from 1626 to 1634 cm^{-1}, with the most pronounced blue shift in SAA_{2-6}.

regions in proteins might help in designing molecules that can prevent and/or disrupt amyloid formation.[41,42]

Results

The suprastructural morphology of amyloid fibers formed by the (all-S) SAA_{1-12} (RSFFSFLGEAFD) peptide is a right-handed helix.[33] Here, we report on the suprastructure of amyloids of truncated segments of the (all-S) SAA_{1-12} peptide {SAA_{2-12} (SFFSFLGEAFD), SAA_{1-11} (RSFFSFLGEAF), SAA_{2-9} (SFFSFLGE), and SAA_{2-6} (SFFSF)} and of two amyloids of the (all-S) SAA_{1-12} mutated peptides {SAA_{1-12}D12A (RSFFSFLGEAFA) and SAA_{1-12}D12L (RSFFSFLGEAFL)}.

Peptides were synthesized by the Fmoc strategy and purified by semipreparative HPLC, and their purity was determined to be more than 97% by analytical HPLC and mass spectrometric analysis (SI Figures 1−3). The amyloids were produced at room temperature in 10% v/v acetic acid at pH 2, as previously described.[35] Amyloid characterization was done by transmission electron microscopy (TEM) thioflavin T (ThT) assay and Fourier transform infrared (FTIR) spectroscopy. All amyloid fibers observed by TEM display several fiber widths in the range of tens of nanometers, whereas fiber lengths vary from hundreds of nanometers up to several micrometers (SI Figure 4).

The truncated peptide amyloids produce the expected spectroscopic shifts distinctive of amyloids in the ThT assay (SI Figure 5). The amide I and II regions of the FTIR spectra of all peptides, truncated and mutated, are characteristic of the β-structure (Figure 1).

The FTIR spectra of SAA_{1-12} and its truncated and mutated peptide amyloids show differences in the position of their main amide I peaks. Relative to SAA_{1-12} and SAA_{1-12} point mutations, the amide I peak of SAA_{2-12} amyloids is red-shifted whereas those of $SAA_{1-11,}$ SAA_{2-9}, and SAA_{2-6} are blue-shifted (Figure 1 and Table 1).

Table 1. Characteristics of the Truncated SAA Peptides Examined

peptide name	peptide sequence	helicity	FTIR amide I position, cm^{-1}	pI
SAA_{1-12}	RSFFSFLGEAFD	100% right-handed	1623	4.67
SAA_{1-12} D12A	RSFFSFLGEAFA	100% right-handed	1624	6.00
SAA_{1-12} D12L	RSFFSFLGEAFL	100% right-handed	1625	6.00
SAA_{2-12}	SFFSFLGEAFD	100% right-handed	1619	4.00
SAA_{1-11}	RSFFSFLGEAF	100% left-handed	1626	6.00
SAA_{2-9}	SFFSFLGE	86% left-handed, 14% right-handed	1626	4.60
SAA_{2-9}, pH 7	SFFSFLGE	100% right-handed	1624	4.60
SAA_{2-9}, pH 7	SFFSFLGE	100% left-handed	1627	4.60
SAA_{2-6}	SFFSF	100% left-handed	1634	5.24

The amyloid suprastructural morphology was determined by high-resolution scanning electron cryo-microscopy (cryo-SEM) for SAA_{1-11}, SAA_{2-12}, and SAA_{2-6} whereas SAA_{2-9} and SAA_{1-12} point-mutated amyloids were examined by (noncryo)-high-resolution SEM. In contrast to TEM, single SEM images can provide information about 3D morphology and are thus appropriate for the determination of helical handedness. Cryogenic sample preparation preserves the hydrated form of biological materials. Additionally, observation at low temperature improves the effective resolution in some of the observed peptides, mainly because the fibers are more resistant to beam damage.

The samples were flash frozen and freeze dried on TEM microscopy grids (Experimental Section). In cases where the residual presence of amorphous ice prevented the clear, easy identification of helicity and handedness, we decided on a statistical sampling of at least 50 independent fibers showing clear helicity from 2 or more independently prepared sample batches. The choice of a sampling of 50 fibers was dictated by the experimental difficulty of the measurements.

SAA_{2-12} (SFFSFLGEAFD) forms helical amyloid fibers. The difference between SAA_{1-12} and SAA_{2-12} amyloids in terms of the peptide sequence consists in the truncation of one arginine (R) from the N terminus. A total of 50 fibers from 2 different fiber batches were visualized in order to determine the chirality of the helical fibers. The observed helicity is right-handed, with 100% of the observed helical fibers having the same handedness (Figure 2). There is, naturally, the possibility that one or more fibers of opposite handedness might have been found had the statistical sampling been wider, but on the basis of previous

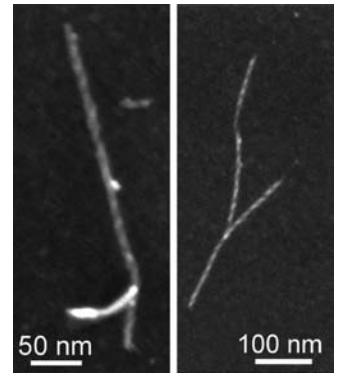

Figure 2. Cryo-SEM micrographs of SAA_{2-12} amyloids showing different fibers, all having right-handed helicity.

(41) Lopez de la Paz, M.; Serrano, L. *Proc. Natl. Acad. Sci. U.S.A.* **2004**, *101*, 87–92.
(42) Gazit, E. *FEBS J.* **2005**, *272*, 5971–5978.

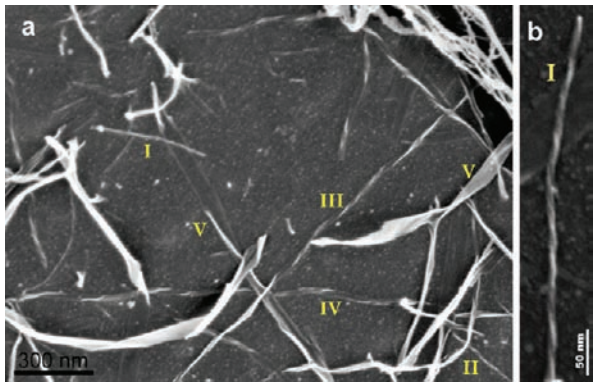

Figure 3. Cryo-SEM micrographs of SAA_{1-11} amyloids: (a) Left-handed chirality that is observed throughout all hierarchical levels of the helical fibers. (b) High-magnification micrograph of fiber I in image a.

experience, we deem the probability low. Fiber widths range from 6.5 to 9 nm with an average of 8 nm. The fiber lengths are in the range of hundreds of nanometers. The right-handed helicity of SAA_{2-12} suggests that its protofilament molecular structure is not a β-sheet, similar to what was found for SAA_{1-12} amyloids. Removal of the N-terminal arginine thus does not appear to affect the suprastructure of the peptide.

In contrast to SAA_{1-12} and SAA_{2-12}, SAA_{1-11} amyloids, formed from the 11 amino acid long peptide (RSFFSFLGEAF), have left-handed helicity. SAA_{2-12} and SAA_{1-11} have the same length (11 amino acids), and the difference between SAA_{1-12} and SAA_{1-11} amyloids consists of the lack of C-terminal aspartic acid (D). A total of 120 helical fibers were visualized in order to determine the handedness of the fibers. Helical fibers widths range between 10 and 30 nm whereas their lengths extend for $\sim$1 μm. All helical fibers are left-handed. At least four different hierarchical levels can be detected under cryo-SEM. Left-handed helicity was observed throughout the four hierarchical levels of the helical fibers (Figure 3a, levels I−IV). A different morphology consists of ribbons with widths in the range of 50 nm, which occasionally randomly twist (Figure 3a, marked V).

SAA_{2-9} amyloids have mostly helical morphology. Ribbon widths range from 55 to 280 nm. Helical fibers show both right-handed and left-handed helicity. A total of 101 helical fibers were visualized from two different fiber batches, 86% (N = 86) of which have left-handed helicity with widths in the range of 34−37 nm and 14% (N = 15) of which have right-handed helicity with widths in the range of 25−26 nm (Figure 4). The distribution was very reproducible in the two independent batches. The fiber lengths are in the range of hundreds of nanometers.

Pentamer (all-S) SAA_{2-6} (SFFSF) was found to be the smallest peptide that forms amyloid fibers (Perugia et al., unpublished results). A total of 55 helical fibers from 3 different fiber batches were visualized in order to determine the chirality of the helical fibers. Under cryo-SEM, different hierarchical levels of fibers were observed, characterized by fiber widths ranging from 7 to 22 nm and fiber lengths extending for several micrometers (Figure 5). The observed helicity is always and only left-handed (i.e., 100% of the observed helical fibers have the same handedness).

Interestingly, microcrystals of the SAA_{2-6} peptides grew spontaneously together with the fibers. The morphology of the SAA_{2-6} crystals under both TEM and SEM appears to be needlelike (Figure 6a,d). The length varies in the range of several micrometers, and the width is <1 μm. Often, fibers emerging

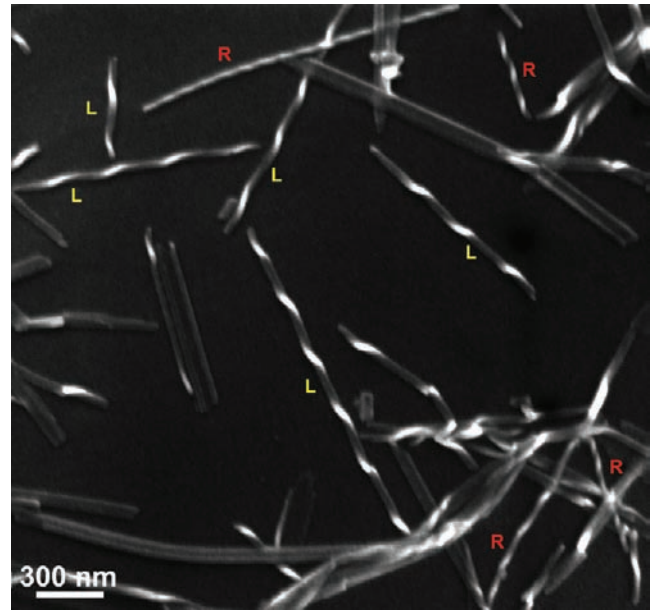

Figure 4. SEM micrograph of SAA_{2-9} amyloid fibers demonstrating the existence of both left-handed (L) and right-handed (R) SAA_{2-9} amyloids.

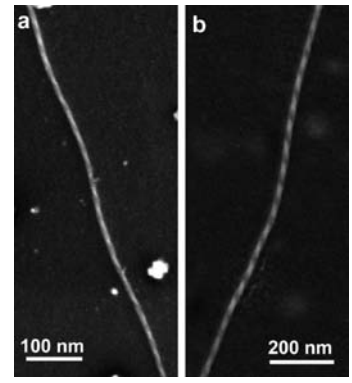

Figure 5. Cryo-SEM micrographs of SAA_{2-6} amyloids demonstrating the left-handed helicity of the fibers at two hierarchical levels.

from the microcrystal tips may be observed, oriented parallel to the long axis of the crystal (Figure 6b,c). This supports the notion that the crystals are derived from the aggregation and crystallization of fibers.

Whether the fibers are the same as we observe individually dispersed on the grid is not clear at this stage. The electron diffraction of the microcrystals yields lattice constants of a = 4.83 Å parallel to the microcrystal axis and b = 22.2 Å perpendicular to it (Figure 6e). The spacing d = 4.83 Å corresponds to the distance between β-strands and is typical of cross-β diffraction common to all amyloids, where β-strands extending perpendicular to the fiber axis are connected by hydrogen bonds oriented along the fiber axis. The spacing d = 22.2 Å may correspond to the distance between alternating β-sheets. The electron diffraction, taken together with the handedness of the fiber suprastructure and with the observation of the fibers emerging from the crystal tips, is consistent with the fibers assuming β-sheet structure.

The difference between SAA_{1-12} and its point-mutated peptides is that the C-terminal aspartic acid was replaced by either leucine (L) in SAA_{1-12} D12L (RSFFSFLGEAFL) or alanine (A) in SAA_{1-12} D12A (RSFFSFLGEAFA), hence these

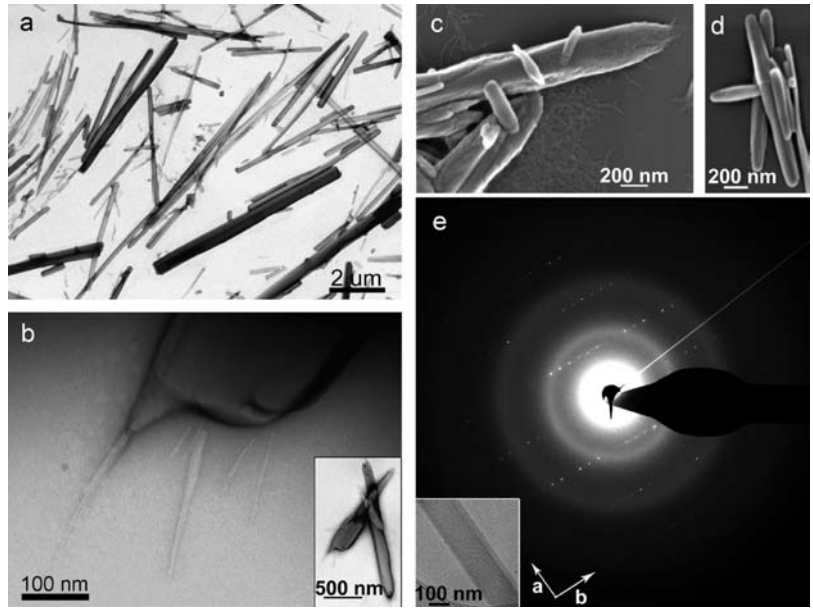

Figure 6. (a) Negatively stained TEM micrograph of the SAA_{2-6} crystals grown spontaneously together with the SAA_{2-6} fibers. (b) Negatively stained TEM micrograph showing amyloid fibers jutting out from the crystal tip. (Inset) TEM micrograph of the same crystal at lower magnification. (c, d) SEM micrographs of SAA_{2-6} microcrystals; the longitudinal surface observed in image d is smooth, whereas the surface in image c is rough and fibers can be noticed to emerge from the tip. (e) Electron diffraction of an SAA_{2-6} crystal. (Inset) Image of the diffracting crystal.

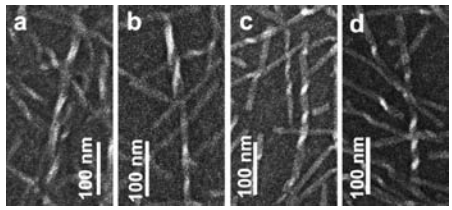

Figure 7. SEM micrograph of SAA_{1-12} D12A (a, b) and SAA_{1-12} D12L (c, d) amyloids demonstrating the right-handed helicity of the fibers. In SAA_{1-11}, SAA_{2-9}, and SAA_{2-6} amyloids, the main amide I peak shifts to higher frequencies (blue shift) ranging from 1626 to 1634 cm^{-1}, with the most pronounced blue shift in SAA_{2-6}.

peptides are devoid of the charge that is contributed by the β-carboxylic moiety of Asp. A total of 54 SAA_{1-12} D12A and 87 SAA_{1-12} D12L helical fibers were visualized. The observed helicity of both mutated amyloids is right-handed, with 100% of the observed helical fibers having the same handedness (Figure 7). The fiber widths of SAA_{1-12} D12A amyloids range between 9 and 29 nm, and those of SAA_{1-12} D12L amyloids range between 6 and 11 nm. It should be kept in mind that this data is based on noncryo-SEM micrographs where the resolution is reduced and the fiber widths do not reflect the width of the hydrated fibers. The fiber lengths are in the range of hundreds of nanometers up to several micrometers. The right-handed helicity of the mutated SAA_{1-12} peptides suggests that their protofilament structure is not a β-sheet, similar to SAA_{1-12}. Point mutation of the C-terminal aspartic acid thus does not appear to affect the suprastructure of the peptide.

Discussion

This is a study case where different segments truncated or mutated from the same SAA_{1-12} peptide form amyloid fibers with different suprastructure chirality indicating differences in their molecular structure organization.

The results obtained are summarized in Table 1, together with the peptide sequences and additional information.

In summary, we found that the helicity of SAA_{1-12} and SAA_{2-12} amyloids and of amyloids of SAA_{1-12} where the C-terminal aspartic acid was mutated to leucine or alanine is exclusively right-handed. The helicity of SAA_{2-9} amyloids is mixed, containing both right- and left-handed fibers. The helicity of SAA_{1-11} and SAA_{2-6} amyloids is exclusively left-handed.

The organization of the cross-β motif into different β-structures, such as a β-sheet, β-helix, or any other β-fold, determines the protofilament structure of amyloids. We believe that the switch in helicity indicates a different protofilament structure. Whereas amyloid fibers with left-handed chirality are compatible with a β-sheet protofilament structure, right-handed helicity rules out the β-sheet structure as a model for the protofilament structure. This is because β-sheets have an intrinsic left-handed twist and helical suprastructures resulting from the association of several β-sheets are expected to display left-handed helicity.[26–30] In globular proteins, β-helix structures were found to form both left- and right-handed helixes. Thus, in principle, the suprastructure of a β-helix cannot be predicted only on the basis of the knowledge of its β-helix structure. It is worthwhile stressing that whereas right-handed fiber helicity does not satisfy the β-sheet protofilament model it does not unequivocally indicate a β-helix structure. It might thus be that the protofilament structure of the right-handed fibers is neither a β-helix nor a left-handed β-sheet.

SAA_{2-6} is a pentapeptide, and it is generally accepted that suprastructures of short peptides are relatively more ordered. Indeed, the average length of β-strands in a β-sheet is 8 amino acids, whereas the smallest known length of a turn of a β-helix structure was found to be in the range of 12 amino acids.[43] Thus, it is very likely that a short peptide such as (all-S) SAA_{2-6} will form a β-sheet simply because there is not enough peptide length to form a whole turn or a loop. Indeed, SAA_{2-6} forms left-handed fibers and crystals that give a diffraction expected for a β-sheet. The 22.2 Å spacing is double the spacing expected

(43) Liou, Y. C.; Tocilj, A.; Davies, P. L.; Jia, Z. *Nature* **2000**, *406*, 322–324.

for juxtaposition between β-sheets; the doubling of cell dimensions may result from the juxtaposition of sheets that are not related by translation along the direction perpendicular to the sheet.[44] The microcrystalline needles spontaneously formed by SAA_{2-6} have unraveled edges from which fibers emerge, remarkably similar to other microcrystals of the same nature, which were studied in depth by Eisenberg and co-workers.[44,45] Sawaya et al. have demonstrated consistently that 13 different amyloidogenic short peptides, 5−7 amino acids long, are amenable to crystallization. The microcrystal cross section does not exceed $2 \times 2\ \mu m^2$, and their morphology is needlelike. The atomic structure of all of these microcrystals was found by X-ray diffraction to be a β-sheet steric zipper.[44,45] Considering that SAA_{2-6} contains three phenylalanines in its short sequence, the β-sheet may be further stabilized by forming the so-called Phe ladder.[46] The Phe ladder may be involved in the stabilization of all of the peptide amyloids examined, independent of the specific β-structure that they assume.

Deducing a full model of the structure of the various SAA amyloid protofilaments is well beyond the scope of this work. A number of remarks can, however, be made concerning the evidence acquired here on the various SAA peptide truncates and mutants.

An interesting correspondence exists between the handedness of the fibers and the position of the main amide I peak in the FTIR spectrum; namely, in all of the right-handed fibers, the amide I peak is red-shifted relative to the left-handed fibers. The amide I peak position is directly correlated to the strength of the hydrogen-bonded network. FTIR spectra cannot in general be used unequivocally to identify β-structure features such as parallel and antiparallel β-sheets or β-sheets and β-helices.[47−49] Several parameters influence the amide I region of the FTIR spectrum, such as the number of β-strands in a β-sheet and the extent of β-sheet twisting.[50] In addition, amide I peak shifts may be also correlated in part to the length of the peptides, with shorter peptides being progressively blue-shifted. We note, however, that both SAA_{1-11} and SAA_{2-12} are 11 amino acids long. Thus, the left-handed helicity observed for SAA_{1-11} amyloids versus the right-handed helicity observed for SAA_{2-12} amyloids, together with the red shift of SAA_{2-12} amyloids, rules out peptide length as a major factor in the change in molecular protofilament structure. A similar red shift of the amide I peak (from 1630 to 1615 cm^{-1}) was observed as a result of the formation of an amyloid structure of transthyretin (TTR) from its β-sheet native structure. This red shift was attributed, on the basis of ssNMR,[51] to different distributions of the ϕ/ψ dihedral angles of the native β-sheet structure relative to those of the amyloid β-structure.[48] The observation of a systematic correlation between fiber helicity and shifts in the amide I peak position thus supports the notion that different molecular β-conformations are involved.

Interestingly, the complex insulin−thioflavin T (ThT) forms two types of nonenantiomeric amyloid fibers with opposite chiral configuration at 40−45 °C, as demonstrated by the extrinsic effect of ThT in induced circular dichroism (ICD).[52] Vibrational circular dichroism (VCD) and Raman optical activity (ROA) have recently proved to be enlightening in the study of amyloid formation and growth.[53,54] These techniques are very sensitive both to molecular and secondary structure chirality. An examination of the SAA-truncated peptides with VCD may thus provide essential information on the correlation between their FTIR band positions and suprastructural chirality.

The suprastructural chirality of truncated segment SAA_{2-12}, where the first arginine from the N-terminus in SAA_{1-12} is absent, is right-handed as in the SAA_{1-12} amyloid. In contrast, the suprastructure of SAA_{1-11} amyloids is left-handed. Thus, the truncation of SAA_{1-12} by one aspartic acid (D) is sufficient to induce a switch in suprastructural handedness, but the truncation of arginine is not. It might be hypothesized that the presence of a charged C-terminus even at the low pH used for amyloid fiber synthesis is responsible both for the red shift in the amide I position and for the formation of head-to-tail peptide chains,[55] inducing a continuous chain structure motif. This could explain why the eight amino acids long peptide SAA_{2-9}, which would be considered well within the range of the β-sheet-forming peptides, still forms, in part, a right-handed structure. However, the amyloids formed by SAA_{1-12} peptides where the acidic C-terminal D has been mutated into the hydrophobic L or A amino acids, also exclusively form right-handed helices, ruling out the possibility that the charge contributed by the β-carboxylic moiety of D at the C-terminus is related to the suprastructure chirality. Interestingly, amyloid helicity correlates to the IR amide I shift over and beyond the effect of possible C-terminal charge, thus the amide I peak in SAA_{1-12} D12L and SAA_{1-12} D12A is located at 1625 and 1624 cm^{-1}, respectively, substantially red-shifted relative to SAA_{1-11}, which has the same PI but forms left-handed helices. Furthermore, preliminary experiments performed on SAA_{2-9} at pH 7 resulted alternatively in the formation of exclusively right-handed or exclusively left-handed helices (data not shown). In agreement with the trend above, the amide I peaks of the right-handed amyloids are red-shifted relative to those of the left-handed amyloids (Table 1). We conclude that although peptide acidity does cause a red shift in the position of the amide I peak, as shown by SAA_{2-12}, the systematic red shift associated only with the fibers with right-handed helicity unequivocally indicates a different structure assumed by these fibers, relative to the β-sheet structure of the left-handed fibers.

Without the need for a high-resolution molecular structure determination, the above demonstrates that any change in peptide sequence and chemistry, even a point mutation, may induce a change in the protofilament structure that is reflected in the fiber suprastructure. Consequently, the structure of the smallest unit

(44) Sawaya, M. R.; Sambashivan, S.; Nelson, R.; Ivanova, M. I.; Sievers, S. A.; Apostol, M. I.; Thompson, M. J.; Balbirnie, M.; Wiltzius, J. J.; McFarlane, H. T.; Madsen, A. O.; Riekel, C.; Eisenberg, D. *Nature* **2007**, *447*, 453–457.
(45) Nelson, R.; Sawaya, M. R.; Balbirnie, M.; Madsen, A. O.; Riekel, C.; Grothe, R.; Eisenberg, D. *Nature* **2005**, *435*, 773–778.
(46) Reches, M.; Porat, Y.; Gazit, E. *J. Biol. Chem.* **2002**, *277*, 35475–35480.
(47) Barth, A.; Zscherp, C. *Q. Rev. Biophys.* **2002**, *35*, 369–430.
(48) Zandomeneghi, G.; Krebs, M. R.; McCammon, M. G.; Fandrich, M. *Protein Sci.* **2004**, *13*, 3314–3321.
(49) Khurana, R.; Fink, A. L. *Biophys. J.* **2000**, *78*, 994–1000.
(50) Barth, A. *Biochim. Biophys. Acta* **2007**, *1767*, 1073–1101.
(51) Jaroniec, C. P.; MacPhee, C. E.; Bajaj, V. S.; McMahon, M. T.; Dobson, C. M.; Griffin, R. G. *Proc. Natl. Acad. Sci. U.S.A.* **2004**, *101*, 711–716.
(52) Loksztejn, A.; Dzwolak, W. *J. Mol. Biol.* **2008**, *379*, 9–16.
(53) Ma, S.; Cao, X.; Mak, M.; Sadik, A.; Walkner, C.; Freedman, T. B.; Lednev, I. K.; Dukor, R. K.; Nafie, L. A. *J. Am. Chem. Soc.* **2007**, *129*, 12364–12365.
(54) McColl, I. H.; Blanch, E. W.; Gill, A. C.; Rhie, A. G.; Ritchie, M. A.; Hecht, L.; Nielsen, K.; Barron, L. D. *J. Am. Chem. Soc.* **2003**, *125*, 10019–10026.
(55) Makin, O. S.; Atkins, E.; Sikorski, P.; Johansson, J.; Serpell, L. C. *Proc. Natl. Acad. Sci. U.S.A.* **2005**, *102*, 315–320.

forming an amyloid structure does not necessarily reflect the full-length protein amyloid structure.

Proteins or peptides forming amyloid fibers are believed to "misfold" into a β-structure because of the inducing activity of short sequences, the so-called amyloid core sequences, having an intrinsic tendency to aggregate into β-structures.[56,44] It has been demonstrated that a point mutation in the core of an amyloidogenic protein inhibits amyloid aggregation.[57,58] Furthermore, the introduction of a small amyloidogenic core in a non-amyloidogenic protein may induce amyloid formation.[59,60]

In enthalpy terms, the amyloid structure is more stable than the globular monomer structure; however, the pathway followed kinetically during the transformation is not always straightforward. In particular, by assuming that misfolding starts from the aggregation of the core sequences, it is not necessarily true that the structure of these cores in the full-length protein amyloids must be identical to that assumed by the isolated shortest amyloid-forming peptide segment. This does not contradict the evidence showing that amyloids formed by short peptides can nucleate the aggregation of longer sequences.[44] The fact that isolated short fragments of SAA containing the same amyloidogenic core sequence fold into different amyloid structures is a good demonstration of this concept. Understanding the effect of small chemical changes on amyloid protofilament structure thus appears to be essential when studying amyloid formation.

Experimental Section

Synthesis of Serum Amyloid A Truncated and Mutated Peptides SAA_{2-12}, SAA_{1-11}, SAA_{2-9}, SAA_{2-6}, SAA_{1-12} D12A, and SAA_{1-12} D12L. SAA truncated and mutated peptides—(all-S) SAA_{2-12} (SFFSFLGEAFD), (all-S) SAA_{1-11} (RSFFSFLGEAF), (all-S) SAA_{2-9} (SFFSFLGE), (all-S) SAA_{2-6} (SFFSF), (all-S) SAA_{1-12} D12A (RSFFSFLGEAFA), and (all-S) SAA_{1-12} D12L (RSFFSFLGEAFl)—were synthesized by the solid-phase method using an Advanced Chemtech APEX 396 multiple peptide synthesizer (Louisville, KY) following the commercial protocol recommended by the manufacturer for the Fmoc strategy. Before each coupling, deprotection of the α-amino group was achieved by reaction with 20% v/v piperidine/DMF solution twice, for 10 and 20 min. After the completion of chain assembly, the peptide was deprotected and cleaved from the polymer (Wang resin (all-S), Novabiochem Laufelfingen, Switzerland)) with a mixture of trifluoroacetic acid (TFA), thioanisole, triethylsilane, and water (85:5:5:5) at room temperature for 3 h. The cleaved peptide was precipitated with ice-cold tert-butyl methyl ether and collected by centrifugation (RT; 2000 rpm). Pellets were washed three times with tert-butyl methyl ether followed by centrifugation, redissolution in DDW, and lyophilization. The crude peptides were purified by semipreparative HPLC, and their purity was determined to be more than 97% by HPLC and mass spectral analysis. (For more information, see the Supporting Information).

Serum Amyloid A Segment Aggregation. All (all-S) serum amyloid A truncated and mutated peptide amyloids were grown in 10% v/v acetic acid at pH 2 for at least 24 h at room temperature as previously described.[35] All amyloids were characterized by scanning electron microscopy (SEM) and FTIR. Truncated amyloids were additionally characterized by transmission electron microscopy (TEM) and thioflavin T (ThT) assay. (For more information, see the Supporting Information).

FTIR. Samples were prepared by evaporating 10 μL drops of a 10 mg/mL suspension of the truncated and mutated peptide amyloid fibers on CaF_2 glass slides. The fibers were resuspended twice in D_2O and subsequently dried. Spectra were measured in a Thermo Scientific Nicolet 6700 FTIR spectrometer equipped with Omnic software using 2 cm^{-1} resolution and the averaging of 128 scans. All spectra were normalized and baseline-corrected.

Transmission Electron Microscopy. Prior to deposition on the grid, the amyloid fiber suspensions were sonicated (30 s) on ice three times and diluted 5−10-fold. Drops (7−10 μL each) were deposited on glow-discharged carbon-coated 400 mesh copper TEM grids for 1 min and blotted. The grids were negatively stained with 2% uranyl-acetate (incubation time 30 s) and observed with a Tecnai-12 (Philips) transmission electron microscope operated at 120 kV. For TEM diffraction, 5 μL of the sample was applied to a 300-mesh copper grid coated with lacey carbon (SPI Supplies). Samples were blotted in an environment of 100% relative humidity and plunged into liquid ethane using a CEVS plunger.[61] Specimens were observed at −180 °C in a Tecnai F20 transmission electron microscope (FEI) operated at 200 kV using a Gatan 626 cryoholder at a temperature of −180 °C. The specimens were observed under low-dose conditions. Images were captured digitally on a TVIPS F224 CCD camera.

Scanning Electron Microscopy. Drops (7−10 μL each) of a sonicated and 1:10 diluted amyloid fiber suspension were deposited onto carbon-coated 400 mesh copper grids and blotted in air to dryness. Grids were coated with 1 to 2 nm of chromium and observed with a high-resolution Ultra 55 SEM equipped with a Schottky field-emission gun (Zeiss, Germany) using an in-lens secondary electron detector.

Scanning Electron cryo-Microscopy. Drops (7−10 μL each) of sonicated and 1:5 to 1:10 diluted amyloid fiber suspensions were deposited on glow-discharged carbon-coated 400 mesh copper TEM grids for 1 min. Grids were blotted, washed twice with 7 μL of Millipore water, blotted again in an environment of 100% relative humidity, and immediately plunge frozen in liquid ethane using a CEVS plunger.[61] The grids were then freeze dried for 3 h at −80 °C in a BAL-TEC BAF 060 freeze-etching system. Grids were coated multidirectionally with 2 nm of chromium. Samples were observed with an in-lens secondary electron detector in a high-resolution Ultra 55 SEM (Zeiss, Germany) at −120 °C.

Acknowledgment. We thank Eyal Shimony from the Electron Microscopy Center at the Weizmann Institute of Science for his constant guidance and support. We also thank Sara Rubinraut and Elena Monticelli for help with peptide synthesis. The electron microscopy studies were conducted at the Irving and Cherna Moskowitz Center for Nano and Bio-Nano Imaging at the Weizmann Institute of Science. We thank the Israeli Science Foundation for support from a grant on converging technologies and the Helen & Milton A. Kimmelman Center for support. L.A. is the incumbent of the Dorothy and Patrick E. Gorman Professorial Chair, and M.F. is the incumbent of the Lester B. Pearson Professorial Chair.

Supporting Information Available: SAA truncated peptide syntheses and amyloid characterization by TEM and ThT assay. This material is available free of charge via the Internet at http://pubs.acs.org.

JA909345P

(56) Tartaglia, G. G.; Pawar, A. P.; Campioni, S.; Dobson, C. M.; Chiti, F.; Vendruscolo, M. *J. Mol. Biol.* **2008**, *380*, 425–436.
(57) von Bergen, M.; Friedhoff, P.; Biernat, J.; Heberle, J.; Mandelkow, E. M.; Mandelkow, E. *Proc. Natl. Acad. Sci. U.S.A.* **2000**, *97*, 5129–5134.
(58) Patel, H.; Bramall, J.; Waters, H.; De Beer, M. C.; Woo, P. *Biochem. J.* **1996**, *318*, 1041–1049.
(59) Ventura, S.; Zurdo, J.; Narayanan, S.; Parreno, M.; Mangues, R.; Reif, B.; Chiti, F.; Giannoni, E.; Dobson, C. M.; Aviles, F. X.; Serrano, L. *Proc. Natl. Acad. Sci. U.S.A.* **2004**, *101*, 7258–7263.
(60) Teng, P. K.; Eisenberg, D. *Protein Eng., Des. Sel.* **2009**, *22*, 531−536.
(61) Bellare, J. R.; Davis, H. T.; Scriven, L. E.; Talmon, Y. *J. Electron Microsc. Tech.* **1988**, *10*, 87–111.